Supporting Information

Tumor Vasculature Targeted Photodynamic Therapy for Enhanced Delivery of Nanoparticles

Zipeng Zhen[1†], Wei Tang[1†], Yen-Jun Chuang[2], Trever, Todd[1], Weizhong Zhang[1], Xin Lin[3], Gang Niu[3], Gang Liu[4], Lianchun Wang[5], Zhengwei Pan[2], Xiaoyuan Chen[3], Jin Xie[1,6]*

[1]Department of Chemistry, University of Georgia, Athens, Georgia 30602, United States

[2]Department of Physics, University of Georgia, Athens, Georgia 30602, United States

[3]National Institute of Biomedical Imaging and Bioengineering (NIBIB), National Institutes of Health (NIH), Bethesda, Maryland 20852, United States

[4]State Key Laboratory of Molecular Vaccinology and Molecular Diagnostics & Center for Molecular Imaging and Translational Medicine, School of Public Health, Xiamen University, Xiamen, 361102, China

[5]Department of Biochemistry and Complex Carbohydrate Research Center (CCRC), University of Georgia, Athens, Georgia 30602, United States

[6]Bio-Imaging Research Center (BIRC), University of Georgia, Athens, Georgia 30602, United States

† These authors contributed equally to this work.

* Address correspondence to jinxie@uga.edu.

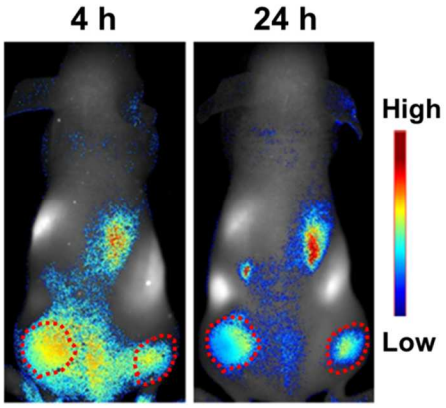

Figure S1. Tumor targeting study with P-RFRTs in bilateral 4T1 tumor models. The tumors were circled by red dashed lines.

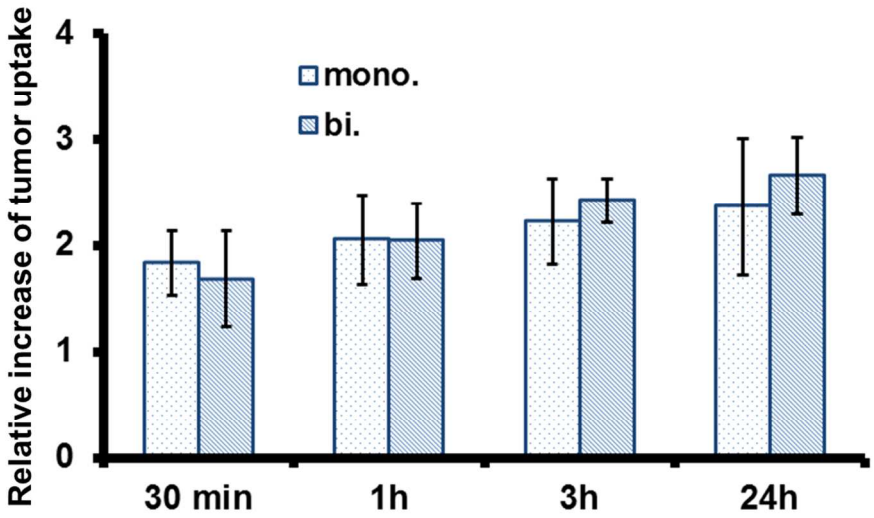

Figure S2. Comparison of relative increase of tumor uptake. The results came from studies performed on 4T1 tumor models bearing either one (mono) or two (bi) tumors.

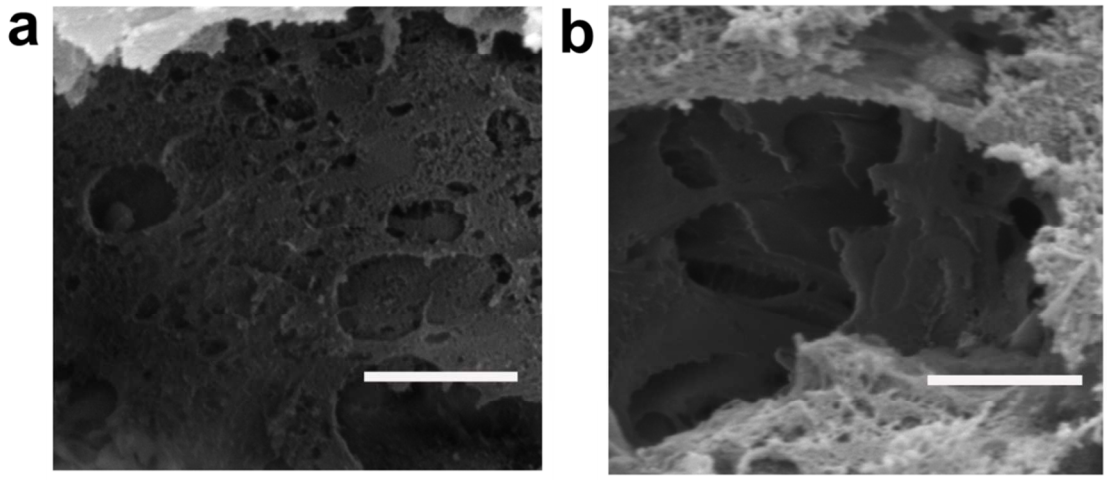

Figure S3. Selected SEM images of tumor vessels with (a) and without (b) PDT treatment. Scale bar, 1 μm.

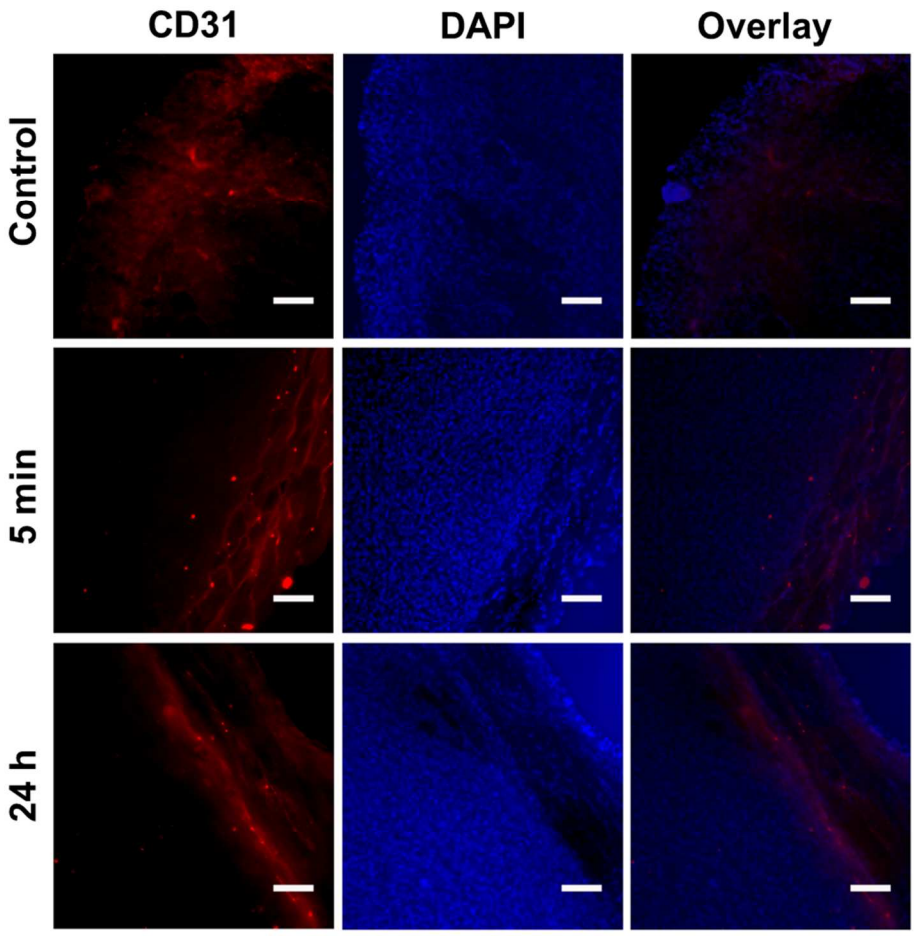

Figure S4: CD31 staining on 4T1 tumor samples taken before (the first row) as well as 5 min and 24 h after P-RFRT-mediated PDT. Tumor vessels were convoluted and irregular before the PDT. After the treatment, however, the vessel became more regular and ordered, more so at 5 min. Red, CD31. Blue, DAPI. Scale bars, 100 μm.

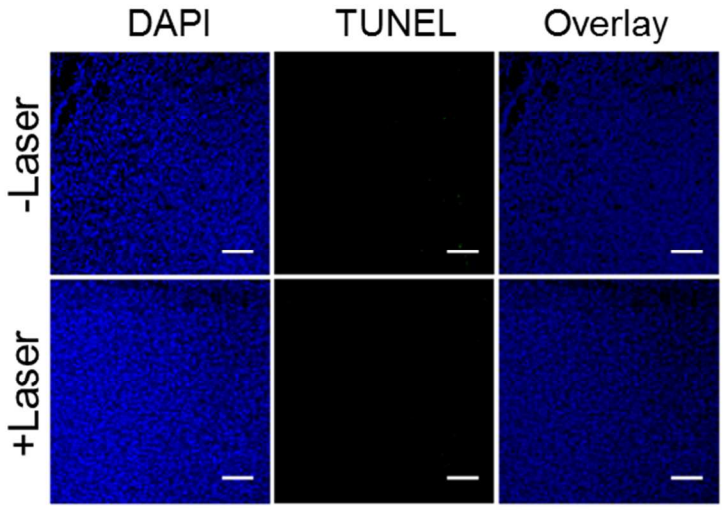

Figure S5: TUNEL assays on samples from irradiated (PDT-treated) and non-irradiated (non-PDT treated) tumors. There was no detection of significantly increased cell death after PDT. Blue, DAPI. Green, TUNEL. Scale bars, 100 μm.

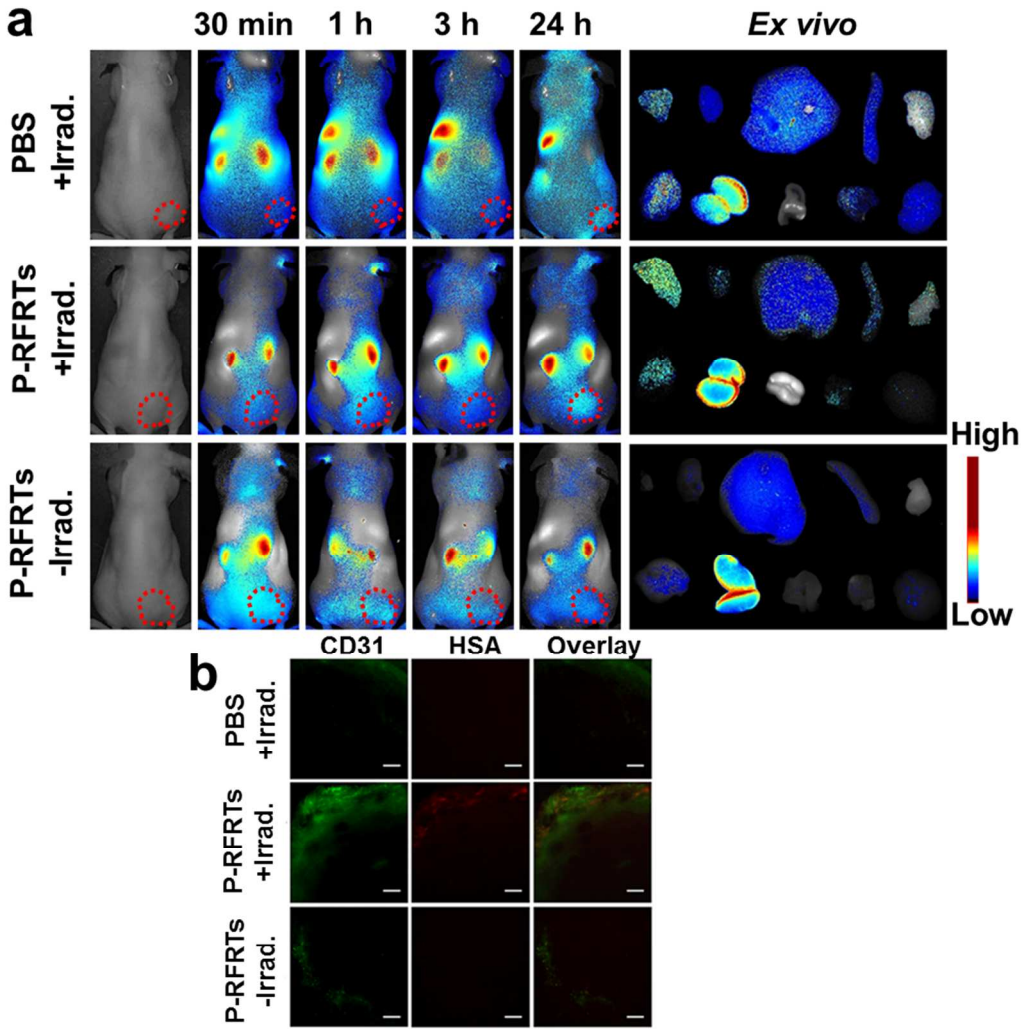

Figure S6: a) *In vivo* and *ex vivo* imaging. The study was performed in PC-3 tumor models. P-RFRTs were i.v. injected first. Photoirradiation was applied to the tumors 24 h later. 5 min after the end of the irradiation, IRDye800 labeled HSA was administered. Control groups received P-RFRTs but no irradiation (the third row) or irradiation only (the first row) before the HSA injection. Fluorescence imaging was performed at 30 min, 1 h, 3 h, and 24 h to evaluate the uptake of the probes by tumors (circled by red dashed lines). After the 24 h imaging, the animals were sacrificed. Tumors as well as major organs were subjected to *ex vivo* imaging to further assess the impact of the PDT on biodistribution of albumins. For each group, the tissues were arranged in the following order: The first row, tumor, heart, liver, spleen and skin; the second row, lung, kidneys, intestine, muscle and brain. b) Histology studies on tumor tissues. More albumins were observed in PDT treated tumors (the second row). Green, CD31. Red, HSA. Scale bars, 100 μm.

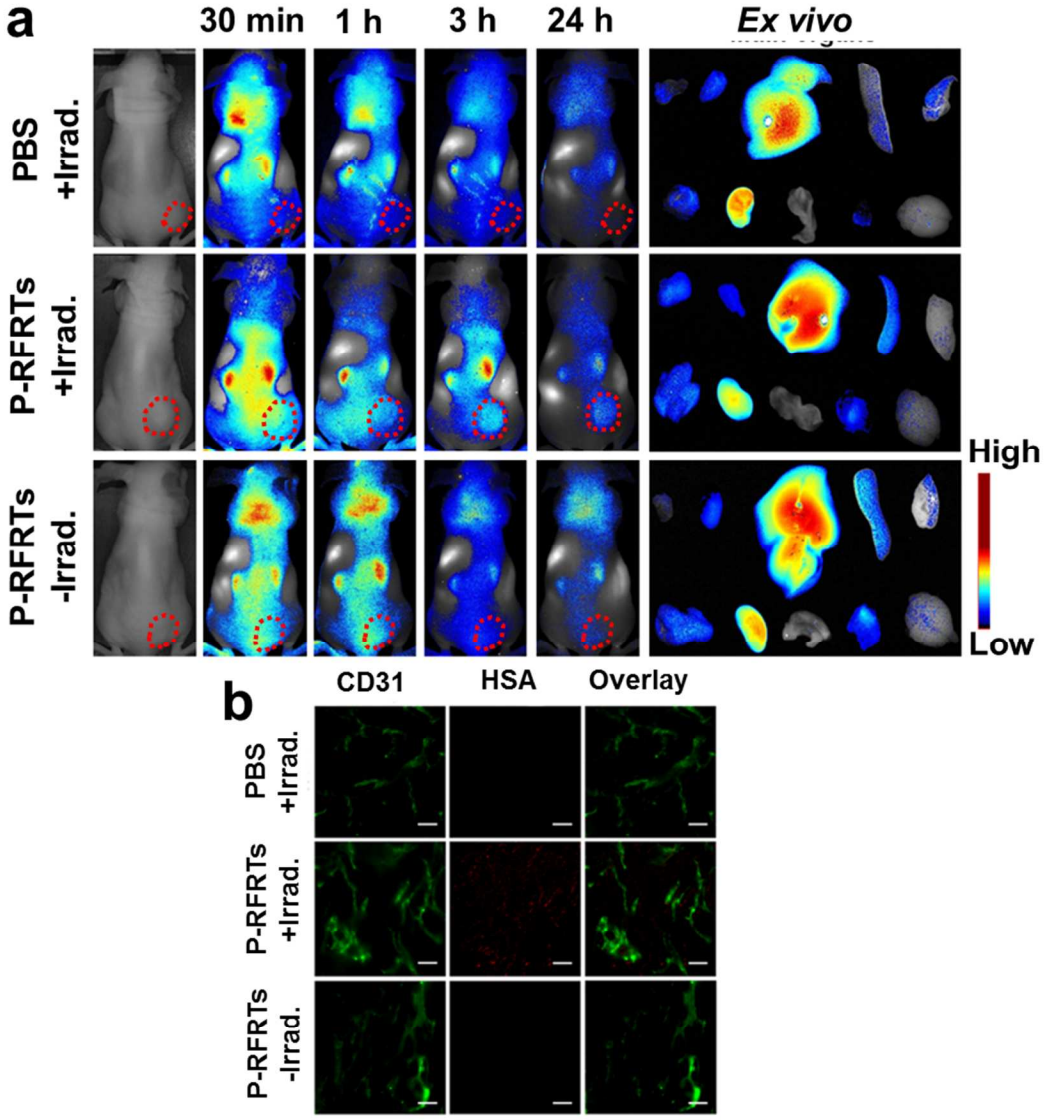

Figure S7: a) *In vivo* and *ex vivo* imaging. The study was performed in MDA-MB-435S tumor models. P-RFRTs were i.v. injected first. Photoirradiation was applied to the tumors 24 h later. 5 min after the end of the irradiation, IRDye800 labeled HSA was administered. Control groups received P-RFRTs but no irradiation (the third row) or irradiation only (the first row) before the HSA injection. Fluorescence imaging was performed at 30 min, 1 h, 3 h, and 24 h to evaluate the uptake of the probes by tumors (circled by red dashed lines). After the 24 h imaging, the animals were sacrificed. Tumors as well as major organs were subjected to *ex vivo* imaging to further assess the impact of the PDT on biodistribution of albumins. For each group, the tissues were arranged in the following order: The first row, tumor, heart, liver, spleen and skin; the second row, lung, kidneys, intestine, muscle and brain. b) Histology studies on tumor tissues. More albumins were observed in PDT treated tumors (the second row). Green, CD31. Red, HSA. Scale bars, 100 μm.

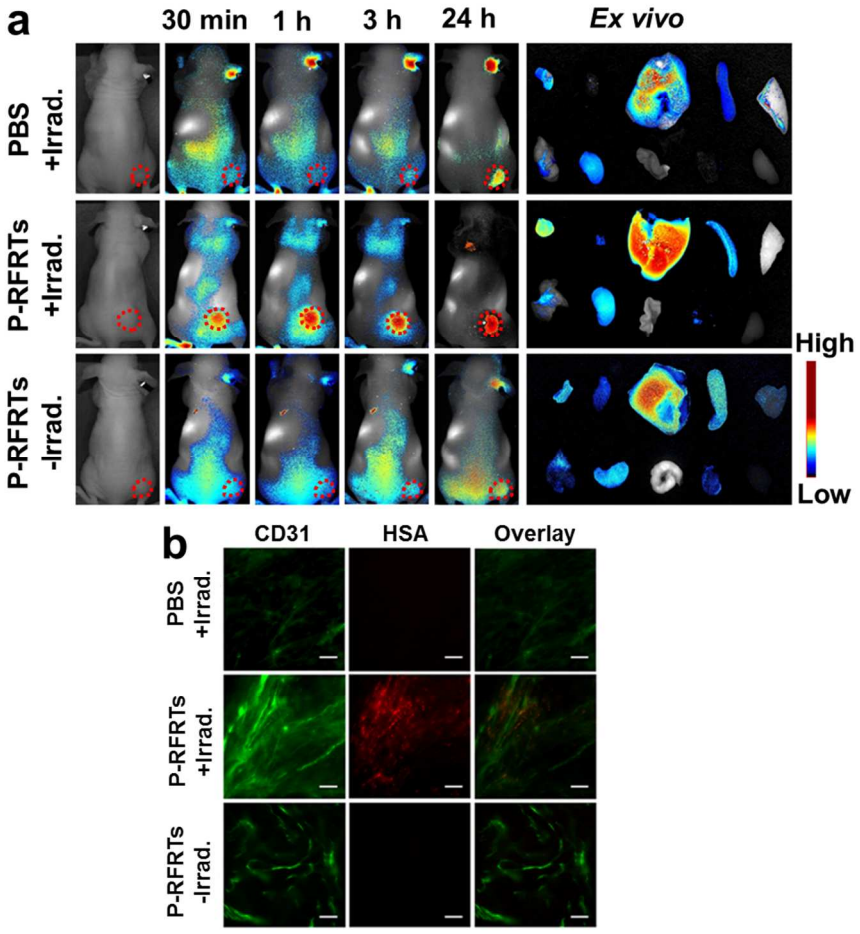

Figure S8: a) *In vivo* and *ex vivo* imaging. The study was performed in U87MG tumor models. P-RFRTs were i.v. injected first. Photoirradiation was applied to the tumors 24 h later. 5 min after the end of the irradiation, IRDye800 labeled HSA was administered. Control groups received P-RFRTs but no irradiation (the third row) or irradiation only (the first row) before the HSA injection. Fluorescence imaging was performed at 30 min, 1 h, 3 h, and 24 h to evaluate the uptake of the probes by tumors (circled by red dashed lines). After the 24 h imaging, the animals were sacrificed. Tumors as well as major organs were subjected to *ex vivo* imaging to further assess the impact of the PDT on biodistribution of albumins. For each group, the tissues were arranged in the following order: The first row, tumor, heart, liver, spleen and skin; the second row, lung, kidneys, intestine, muscle and brain. b) Histology studies on tumor tissues. More albumins were observed in PDT treated tumors (the second row). Green, CD31. Red, HSA. Scale bars, 100 μm.

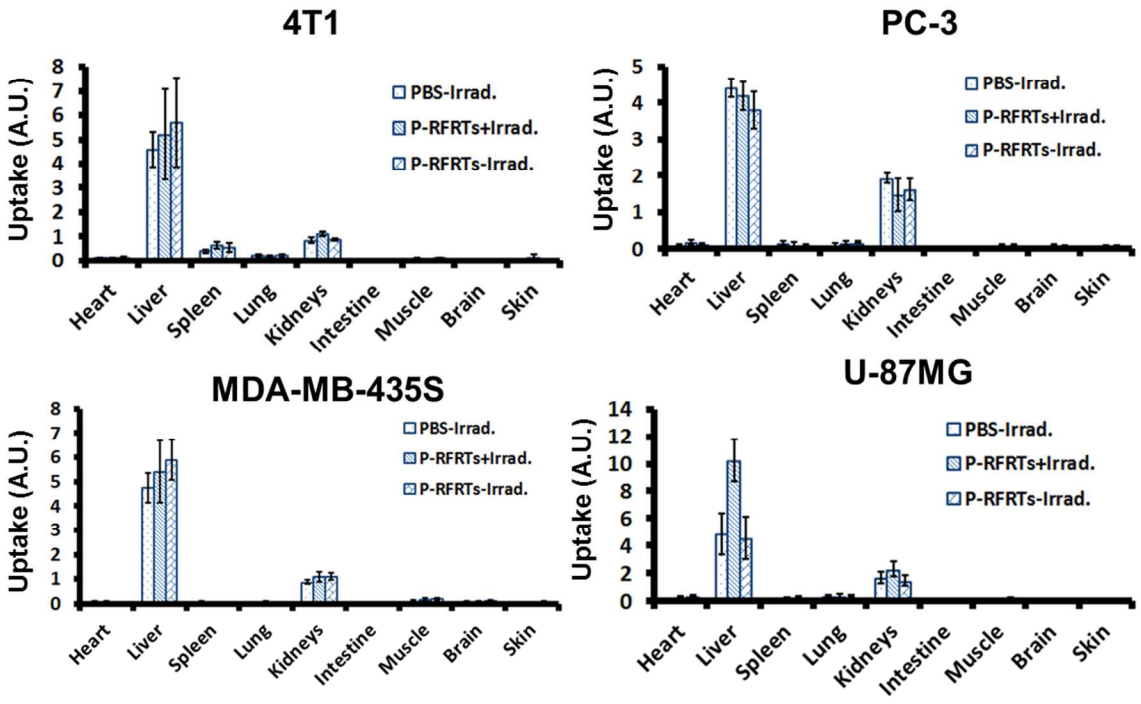

Figure S9: Histogram comparison of accumulation of albumins in normal tissues. The results were based on ROI analyses on *ex vivo* imaging data (from Fig. 2c and Supplementary Fig. S5-7).

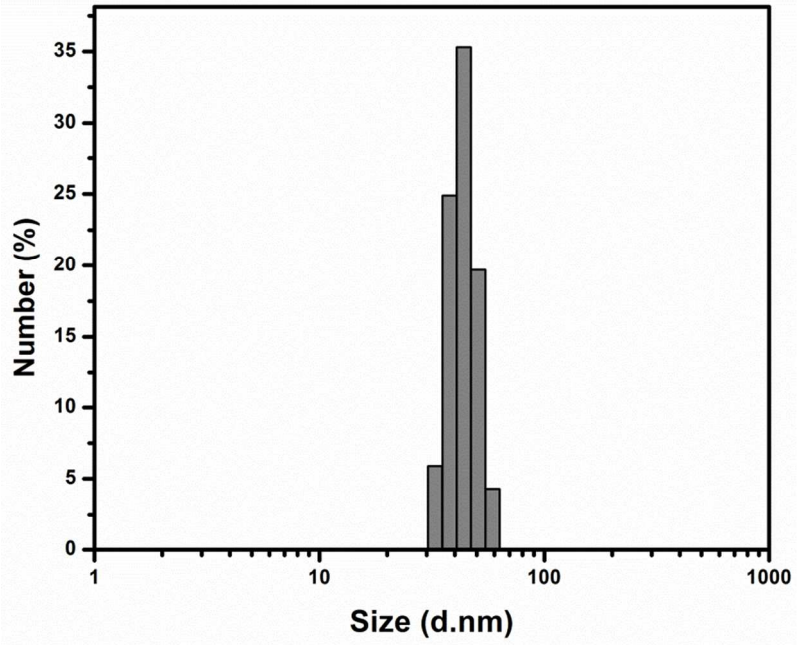

Figure S10. Hydrodynamic size of QDs, measured by DLS. The average size is 43.23 ± 6.27 nm.

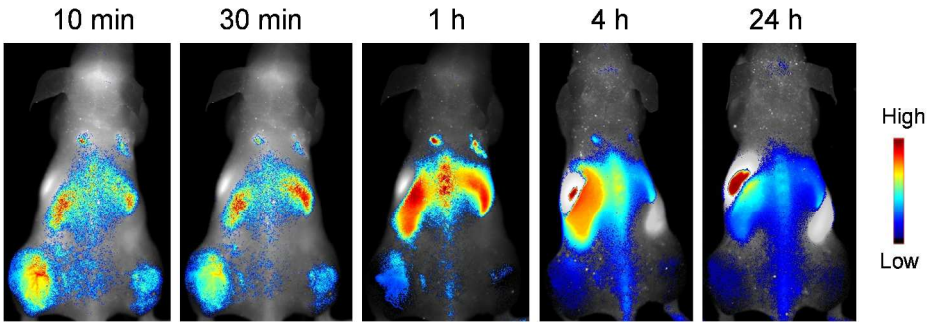

Figure S11. *In vivo* images taken at different time points after QD injection. P-RFRTs were injected first and irradiation was only applied to the left-side tumors. QDs were injected after the end of irradiation.

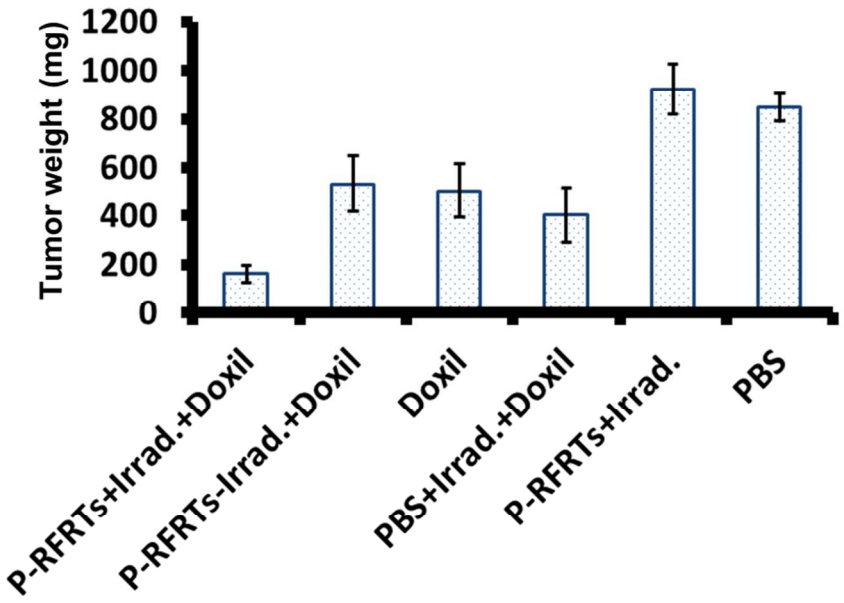

Figure S12: Histogram comparison of tumor weights among different therapy groups.

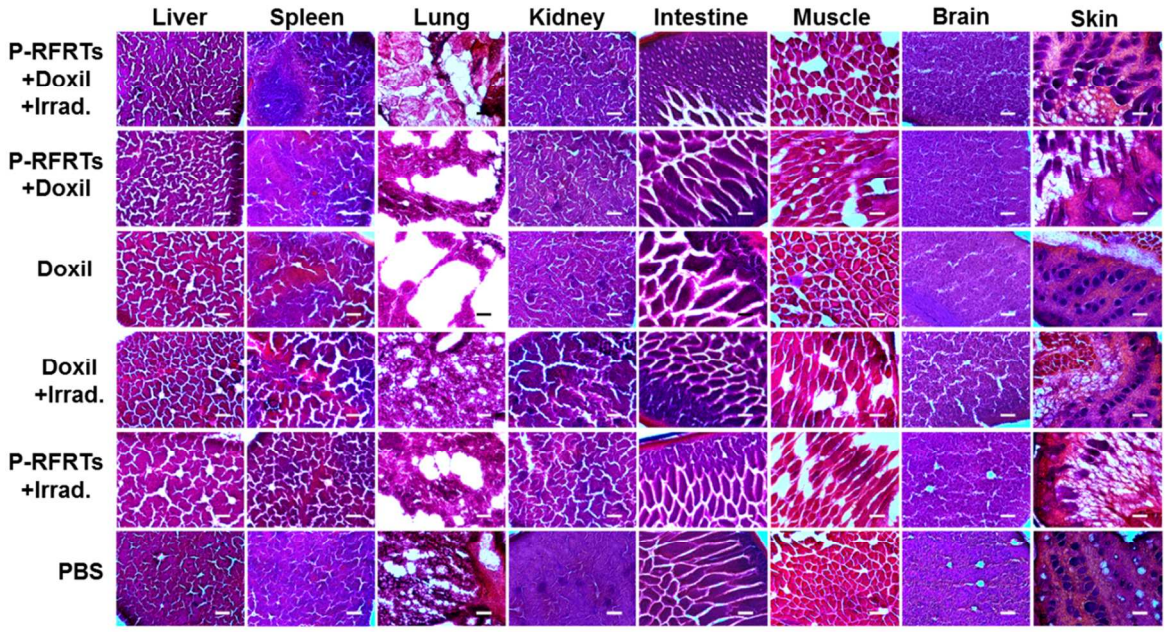

Figure S13. H&E staining on normal tissues from different therapy groups. No significant difference was observed between the group receiving the combination therapy (the first row) and the others receiving Doxil. Scale bars, 100 μm.

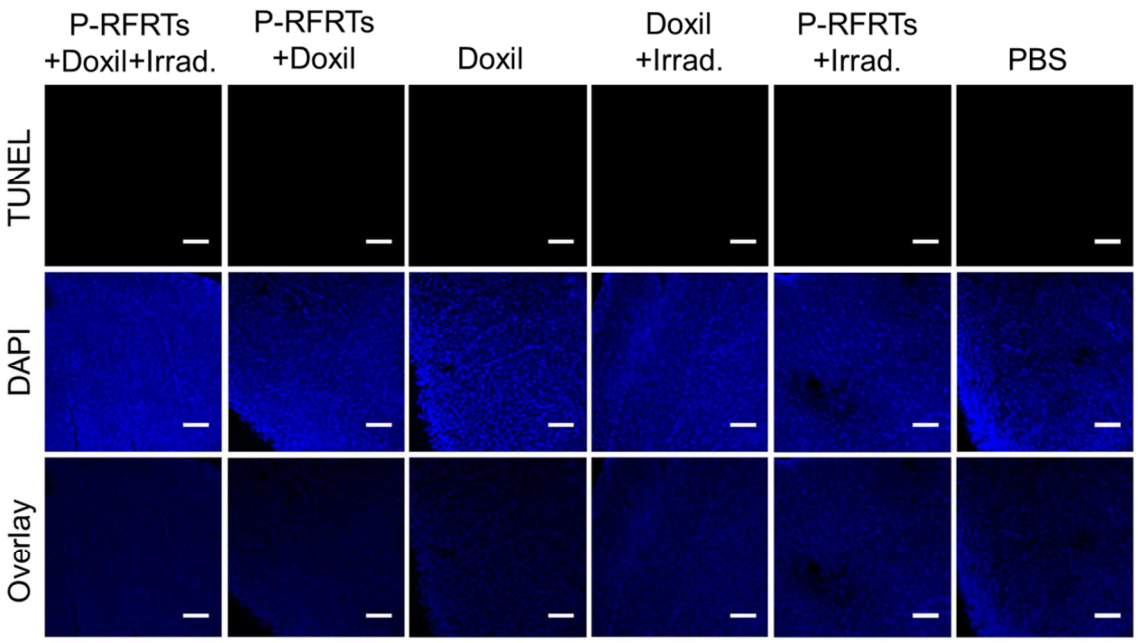

Figure S14: TUNEL assays with heart tissue samples from different therapy groups. Blue, DAPI. Green, TUNEL. Scale bars, 100 μm.